NGU REPORT
2017.018

Dynamic modelling with DAN3D of Stampa scenario 3A

GEOLOGY FOR SOCIETY
SINCE 1858

GEOLOGICAL
SURVEY OF
NORWAY
- NGU -

GEOLOGICAL SURVEY OF NORWAY
- NGU -

Geological Survey of Norway
P.O.Box 6315 Sluppen
NO-7491 TRONDHEIM
Tel.: 47 73 90 40 00

REPORT

Report no.: 2017.018

ISSN: 0800-3416 (print)
ISSN: 2387-3515 (online)

Grading: Open

Title:
DYNAMIC MODELLING WITH DAN3D OF STAMPA SCENARIO 3A

Authors:
Ivanna Penna, Martina Böhme, Reginald Hermanns

Client:
Norwegian Water Resources and Energy Directorate (NVE)

County:
Sogn og Fjordane

Commune:
Aurland

Map-sheet name (M=1:250.000)

Map-sheet no. and name (M=1:50.000)

Deposit name and grid-reference:
Stampa Scenario 3A

Number of pages: 16 **Price (NOK):** 60
Map enclosures:

Fieldwork carried out:

Date of report:
13.03.2017

Project no.:
310100

Person responsible:

Summary:
The unstable rock slope at Stampa (Aurland Municipality; Sogn og Fjordane), is among the largest unstable rock slopes in Norway. It has been investigated over more than a decade in detail and several scenarios have been defined for potential failure. One of those (scenario 3A, also called Joasetbergi) has recently been defined as a high risk site that requires continuous early warning. The main goal of the work outlined in this report was to model the run-out dynamics of a potential failure of this high risk scenario. The dynamic modelling was carried out with the software DAN3D, that is widely used to model the motion of highly mobile landslides. The results obtained with the DAN3D software were compared to the Flow-R run-out model, which is the software used by NGU for all unstable rock slope in Norway. We have defined 39 plausible propagation models by selecting a wide range of plausible input parameters.
The results of the dynamic models showed the propagation of materials down to the fjord floor (80 m b.s.l), and impact velocity in the order of 50-70 m/s. The model runs with higher pore pressure coefficients and lower friction angles presented longer run-outs and higher propagation velocities. Previous ground based InSAR surveys carried out by NVE have shown a relationship between displacement rates of the scree deposits covering the slope and weather conditions. The outcomes of those studies suggest that models involving pore pressure close to saturation reflect best the real situation in case of failure. Model runs allowing entrainment of material on the flow path indicate that the failed rock mass can entrain debris from the slope, and the deposited volume turned to be on average 31% higher than the initial one. The results obtained in this study are realistic and match with previous models done in the area. However, their accuracy could be improved if a back analyses on a representative rock slope failure could be done, however well documented historical or prehistorical cases are missing in the area. In addition, the accuracy of the models could be improved by addressing e.g. interactions between the failed rock mass and the vegetation coverage, which in the study area is dense. Future software improvements addressing such information might lead to better constrain the landslides dynamics and its related entrainment process.

Keywords: Unstable slope	Stampa	Joasetbergi
Sogn og Fjordane	Run-out analysis	DAN3D
Flow-R		

TABLE OF CONTENTS

1. INTRODUCTION

Large slope failures constitute a major direct and indirect geohazard in Norway (e.g. Harbitz et al., 2014; Blikra et al., 2016; Hermanns et al., 2016). In addition to the direct impacts of landslides in their propagation areas, when falling into fjords they can also trigger displacement waves with deadly consequences. In the 20th century, slope failures triggered waves that resulted in significant economic and life losses (for example, Loen, 1905 and 1936, and Tafjord, 1934). Past events are not exceptions; Norway counts with a significant number of currently active unstable rock slopes developed on fjord's flanks (NGU, 2017).

In the last two decades, NGU has been analyzing the spatial and temporal distribution of unstable slopes and past slope failures in terms of their main controls and dynamics. Recently, NGU has set up a methodology to quantify the potential direct and indirect consequences of failures, which allows to determine the degree of risk at each site and its related scenarios (Oppikofer et al., 2016; NGU, 2017). Stampa, located at the southern end of Aurlandfjord (Aurland Municipality, Sogn og Fjordane), is one of the largest unstable rock slopes in Norway, that developed in highly deformed phyllitic rocks (Braathen et al., 2004; Hermanns et al., 2011; Böhme et al., 2013). A high-resolution digital elevation model (DEM) and detailed bathymetric data show that past failures detached from the eastern flank of Aurlandfjord deposited significant amount of debris at water depths of 80-100 m (Blikra et al., 2006). The presence of the rockslide deposits highlights the potentiality of failures and consequent displacement waves to impact the fjord in the vicinity of Flåm.

Stampa is an outstanding site and has been a great concern for various institutions. Therefore, several detailed studies have been carried out in the past (e.g. Domaas et al., 2002; Braathen et al., 2004; Blikra et al., 2013; Böhme et al., 2013; Kristensen and Anda, 2016; among others). A recent characterization of the site by NGU has divided the unstable slope into several scenarios. Two of these, scenarios 3A (also called Joasetbergi) and 3B, were defined as having an annual probability of failure of 1/1000-1/100 (Blikra et al., 2016). The scenario 3B was classified as low risk because even if its degree of hazard is high, the propagation of the rock mass will most likely not affect people, buildings or other infrastructure. The scenario 3A was classified as a high risk because of its relatively high likelihood of failure and high potential consequences if the rock mass falls into the fjord, triggering displacement waves. The aim of the research presented here is to produce more detailed information about the dynamics of the rock mass in case of failure of the scenario 3A, as well as its interaction with the substratum from the detachment down to the fjord floor (Figure 1). The dynamic modelling of the potential failure was carried out with the software DAN3D (McDougall and Hungr, 2004). This software has shown to be able to successfully model the motion of highly mobile landslides through back and forward analyses (Sosio et al., 2008; Penna et al., 2013; Schleier et al., 2016, among many others).

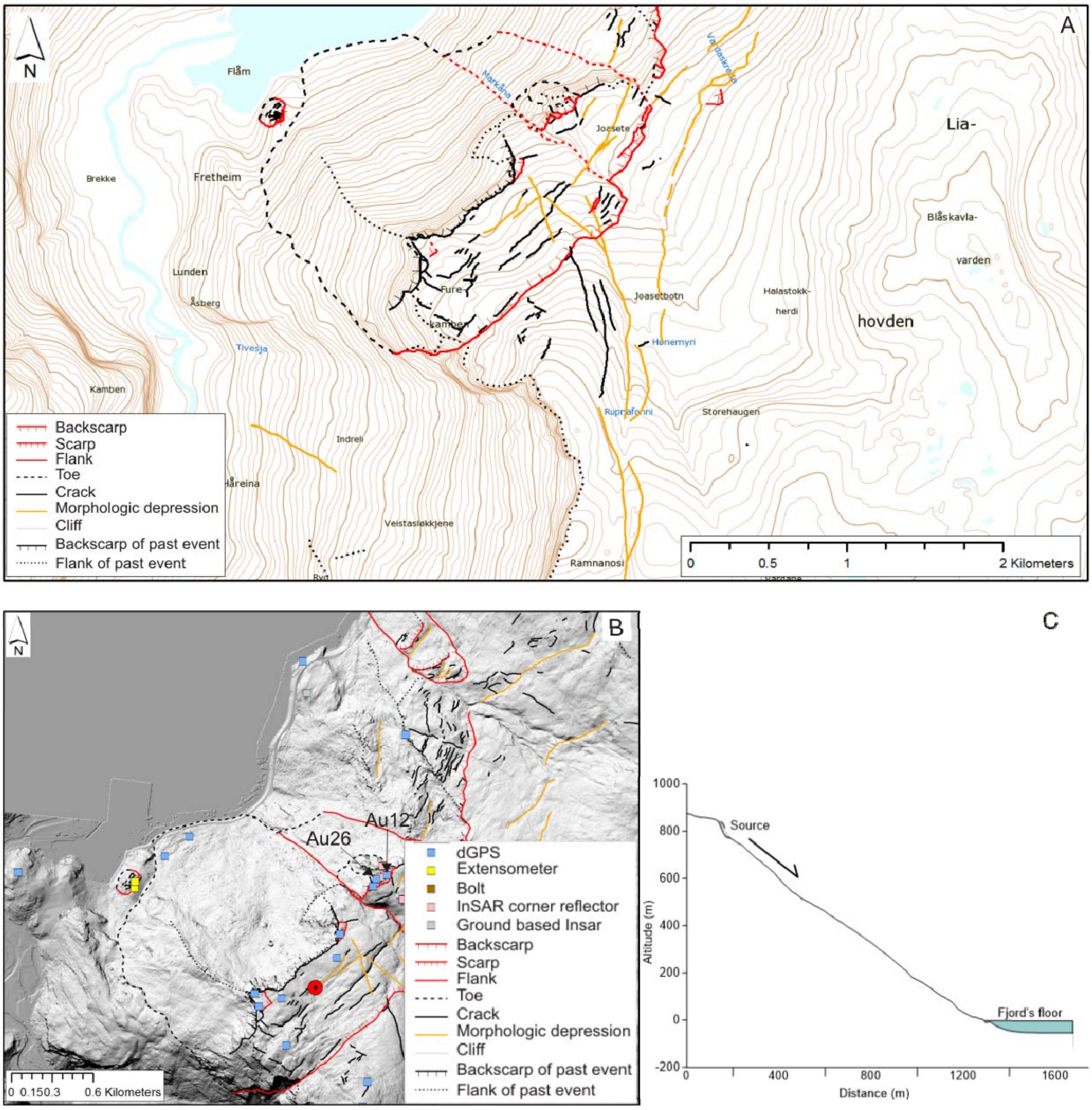

Figure 1. A) Topographic map of Stampa and main slope deformation-related features (NGU, 2017). B) Hillshade map of Stampa, main features and monitoring stations set up on the site. C) Cross section from the source of scenario 3A to floor of Aurlandfjord.

2. GENERAL SETTING AND BACKGROUND INFORMATION

The main geologic and geomorphologic features of the area as well as a description of Stampa scenario 3A are summarized below. More detailed geological background information can be found in Braathen et al. (2004), Hermanns et al. (2011), Böhme et al. (2013), Blikra et al. (2013) and NGU (2017).

2.1 Geologic setting

The eastern flank of Aurlandfjord shows evidences of gravitational deformation from Ramnanosi to Joasete and further north to Otnes (Figure 1; Braathen et al., 2004; Blikra et al., 2006; Böhme et al., 2013). Slope deformation involves Lower Paleozoic and Precambrian phyllite and mica schist. Rocks were strongly deformed during the Caledonian orogeny and thrusted over Precambrian basement. Folds range from centimeter to meter scale (Böhme et al., 2013). Major fractures present NE-SW and WNW-ESE orientation and high angles (ca. 80°). Foliation dips range between 16° to 35° towards the SW. In addition to the metamorphic rocks, the fjord flank presents a thick cover of scree deposits with an estimated thickness of around 50 m based upon geophysical data and topographic reconstructions (Blikra et al., 2013). Detailed studies carried out downslope from Ramnanosi (Figure 1), show that the scree deposits rest over permeable glacial till, which is in turn lying over the bedrock (Domaas et al., 2002).

2.2 Landscape conditions and slope deformation

Past glaciations have left a strong imprint in the landscape of Sogn og Fjordane county. U-shaped valleys, led to fjords with steep walls, such as Aurlandfjord. Glacial retreat gave place to debuttressing and isostatic rebound, that have been suggested as contributing factors for slope instabilities in western Norway (Blikra et al., 2006).

Stampa is characterized by large and continuous open cracks on the upper and middle part of the fjord flank. Main open cracks observed on the surface developed along fractures generated during the Caledonian orogeny. NE-SW joints constitute, in most cases, the back-scarp of the deformation zones, while lateral limits are controlled by WNW-ESE joints. Because of the changing orientation of main structures, Böhme et al. (2013) concluded that failure is better explained by a complex mechanism of deformation rather than a simple one. The deformation rates have been measured by NGU with GNSS since 2005. In 2013, corner reflectors for InSAR monitoring were set up as well, and NVE has been conducting a continuous monitoring with ground-based InSAR since 2011. Displacement rates mostly range between 1.5-4 mm/y, except for scenario 3A (5.5-9.5 mm/y), scenario 3B (north of Joasete; ca. 15 mm/y), and at a GPS point at Bjønnbasen where the displacement rate is 7.4 mm/y (NGU, 2017).

In addition to the current deformation, high-resolution topographic data highlights the occurrence of past failures both above and below the shoreline. Above the shoreline past failures are recognized by the presence of a thick cover of metric-scale angular boulders, and the presence of NE-SW oriented cliffs related to past detachments. On the fjord floor past failures are observed as lobate deposits with hummocks and large-scale boulders on the surface (Blikra et al., 2002; Blikra et al. 2006). The submarine deposits occur at depths of around 100 m in Aurlandfjord. The deposits immediately below Joasetbergi (Figure 1) are 4300 years old, according to surface exposure dating using cosmogenic nuclides on samples extracted from the rockslide deposit (Böhme et al., 2013).

2.3 Stampa scenario 3A (Joasetbergi)

The Stampa scenario 3A (also called Joasetbergi) comprises a volume 280000 m^3 of phyllitic rocks (Figure 1; Böhme et al., 2013). The back-scarp is located 850 m a.s.l, and is around 15 m wide and 30 m long. The limits of this unstable rock mass are controlled by two main sets of structures: the back-scarp coincides with a set oriented NE-SW and the lateral limits coincide with a set oriented WNW-ESE. The frontal part of the unstable rock mass ends in a steep cliff and the foot is located 740 m a.s.l.

GPS measurements on two points (AU 12 and AU 26 on Figure 1) show displacement rates of 5.5-9.5 mm/y between 2005 and 2016. Most of the displacement takes place in the horizontal component, with displacement directions of 270° (GPS point AU-26) and 300° (GPS point AU-12; NGU, 2017).

Downslope from scenario 3A, the fjord flank is covered by dense vegetation and scree deposits that shows creeping movement. Using ground-based InSAR, NVE has measured displacements of 10 to 40 mm in around 8 months in the scree deposits (Kristensen and Anda, 2016).

During the characterization of the site, NGU has modelled the potential propagation of the rock mass and its impact velocity, following the methodology established in Oppikofer et al. (2016). The propagation area extends from Joasetbergi down to the fjord (underwater displacement was not assessed) and has a width of ca. 430 m at the shoreline (NGU, 2017). The run-out velocity obtained with Flow-R is 55-65 m/s, similar to the value obtained with the VAW model (60 m/s) for the velocity of impact.

3. METHODOLOGY

To model the potential propagation of the rock mass involved in Stampa scenario 3A, we used the DAN3D software (McDougall and Hungr, 2004). DAN3D requires as input data: 1) the thickness of the sliding mass (source), a path topography, and a map of materials along the propagation area; 2) control parameters, and; 3) rheological parameters (McDougall and Hungr, 2004; Hungr and McDougall, 2009). In the following sections we summarize the procedures carried out to obtain and select the necessary information.

3.1 Source, topography and properties along the propagation area

The limits of the scenario 3A were defined from interpretation of high resolution DEMs, aerial orthophotos, and field surveying (Böhme et al., 2013). Böhme et al. (2013) computed the volume of scenario 3A by reconstructing potential basal failure surfaces using a high resolution digital elevation model. The procedure followed the methodology proposed by Oppikofer (2009). The volume was estimated in 280000 m^3.

Once the sliding surface is reconstructed, the two key input files (source and path topography) for the DAN3D models can be obtained. The source is the thickness of the unstable rock mass and the path topography is the relief along which the rock mass will displace and interact with the substratum. The path topography results from the subtraction of the current DEM and the modelled thickness of the unstable rock mass. Along the propagation area, three materials were considered: 1) thick colluvium and finer sediments in the lower part, 2) thick colluvium, phyllite with graphite on the middle part, and 3) phyllite with graphite on the upper part of the slope (Table 1).

3.2 Input parameters for the dynamic modelling

The control parameters refers to the number of particles (higher amount, higher resolution of the method), smoothing coefficient of particles, which relates to the smoothness of the interpolated flow depth, and velocity smoothing coefficient (the influence of the neighboring particles on the central particle). For our models we used 2000 particles and no smoothing coefficients.

A combination of Frictional rheology (for the subaerial sector) and Voellmy rheology (for the submerged sector) were used for the dynamic models (Table 1). The combination of both rheologies has proven to be useful to model landslides propagating into water bodies (Mazzanti and Bozzano, 2010; Mazzanti et al., 2011). The parameters of the Voellmy rheology (i.e. friction coefficient, turbulence parameter and a reduction of unit weight) account for the dynamics on the submerged sectors as used above-mentioned studies.

The correct selection of rheological parameters is best based upon the back-analyses of a previous event. For Stampa, there is a lack of information of the location and extension of past detachments, as well as the primary extension and thickness of the deposits. Therefore, no accurate back-analyses could be done. In order to overcome the lack of accurate calibration, a wide range of boundary conditions was used.

We defined 13 model setups with changing conditions on the subaerial part (Frictional rheology) and fixed parameters on the submerged part (Voellmy rheology). The 13 setups were defined by selecting friction angles ranging from 21°-32° and internal friction angles from 23°-32°. In addition, three different pore pressure coefficients (ranging from dry to saturation) were used on each of the 13 setups (39 models in total; Table 1). The limits of the range of parameters were set by considering back-analyses done in other mountain settings (e.g. Hungr and Evans, 1996; Sosio et al., 2008). Entrainment of materials (erosion) was considered along the path on the subaerial sector. The erosion rate (bed-normal depth eroded per unit flow depth and unit displacement; McDougal and Hungr, 2004) was calculated in $0.0021^{1/m}$.

Table 1. Parameters selected for the dynamic models.

Model	Runout conditions	Material Number	Rheology	Unit Weight (kN/m^3)	FA (deg)	FC	t (ms^{-2})	IFA (deg)	Pu		
									Eia	Eib	Eic
E1	Submerged	Material 1	Voellmy	25		0.2	250	32			
	Subaerial	Material 2	Frictional	25	24			29	0	0.5	0.7
		Material 3	Frictional	27	24			29	0	0.5	0.7
E2	Submerged	Material 1	Voellmy	25		0.2	250	32			
	Subaerial	Material 2	Frictional	25	29			29	0	0.5	0.7
		Material 3	Frictional	27	29			29	0	0.5	0.7
E3	Submerged	Material 1	Voellmy	25		0.2	250	32			
	Subaerial	Material 2	Frictional	25	32			29	0	0.5	0.7
		Material 3	Frictional	27	32			29	0	0.5	0.7
E4	Submerged	Material 1	Voellmy	25		0.2	250	32			
	Subaerial	Material 2	Frictional	25	24			25	0	0.5	0.7
		Material 3	Frictional	27	24			25	0	0.5	0.7
E5	Submerged	Material 1	Voellmy	25		0.2	250	32			
	Subaerial	Material 2	Frictional	25	29			25	0	0.5	0.7
		Material 3	Frictional	27	29			25	0	0.5	0.7
E6	Submerged	Material 1	Voellmy	25		0.2	250	32			
	Subaerial	Material 2	Frictional	25	32			25	0	0.5	0.7
		Material 3	Frictional	27	32			25	0	0.5	0.7
E7	Submerged	Material 1	Voellmy	25		0.2	250	32			
	Subaerial	Material 2	Frictional	25	24			27	0	0.5	0.7
		Material 3	Frictional	27	24			27	0	0.5	0.7
E8	Submerged	Material 1	Voellmy	25		0.2	250	32			
	Subaerial	Material 2	Frictional	25	29			27	0	0.5	0.7
		Material 3	Frictional	27	29			27	0	0.5	0.7
E9	Submerged	Material 1	Voellmy	25		0.2	250	32			
	Subaerial	Material 2	Frictional	25	32			27	0	0.5	0.7
		Material 3	Frictional	27	32			27	0	0.5	0.7
E10	Submerged	Material 1	Voellmy	25		0.2	250	32			
	Subaerial	Material 2	Frictional	25	24			23	0	0.5	0.7
		Material 3	Frictional	27	24			23	0	0.5	0.7
E11	Submerged	Material 1	Voellmy	25		0.2	250	32			
	Subaerial	Material 2	Frictional	25	29			23	0	0.5	0.7
		Material 3	Frictional	27	29			23	0	0.5	0.7
E12	Submerged	Material 1	Voellmy	25		0.2	250	32			
	Subaerial	Material 2	Frictional	25	32			23	0	0.5	0.7
		Material 3	Frictional	27	32			23	0	0.5	0.7
E13	Submerged	Material 1	Voellmy	25		0.2	250	32			
	Subaerial	Material 2	Frictional	25	21			29	0	0.5	0.7
		Material 3	Frictional	27	21			29	0	0.5	0.7

FA= Friction Angle (degrees); FC= Friction coefficient (dimensionless); t= Turbulence (m/s^2); IFA= Internal friction angle (degrees); Pu= pore pressure coefficient (dimensionless).

4. RESULTS

The dynamic run-out modelling of Stampa scenario 3A showed that in most cases, a total collapse of the ca. 280000 m^3 would imply the debris reaching the fjord (Figure 2). The rock mass would travel around 1400 m; starting at 850 m a.s.l. in Joasetbergi to 80 m b.s.l. at the fjord floor.

4.1 Run-out distances and entrainment – influence of parameters

Our results show that pore pressure (pu) is a key parameter governing run-out distances. Entrainment increased with increasing saturation of materials. Run-out distances and volumes into the fjord also increased with decreasing friction angles (FA; Table 2; Figure 2).

Table 2. Results of the models carried out with DAN3D. Volumes displaced, entrainment and deposited on the fjord floor.

Model	Final volume (m^3)	Entrainned volume (m^3)	Volume entering fjord (m^3)	Average final volume (m^3)	Average entrainned (m^3)	Average volume entering fjord (m^3)
E1a	352000	74000	202000	334000	56000	121000
E2a	334000	56000	96000			
E3a	326000	49000	24000			
E4a	350000	73000	213000			
E5a	332000	54000	93000			
E6a	323000	46000	26000			
E7a	351000	73000	206000			
E8a	333000	55000	92000			
E9a	325000	48000	21000			
E10a	353000	76000	226000			
E11a	278000	<1000	91000			
E12a	323000	45000	26000			
E13a	357000	79000	258000			
E1b	366000	89000	301000	363000	85000	286000
E2b	363000	85000	284000			
E3b	360000	83000	275000			
E4b	365000	87000	295000			
E5b	361000	83000	278000			
E6b	360000	82000	273000			
E7b	366000	89000	298000			
E8b	362000	84000	282000			
E9b	359000	82000	271000			
E10b	364000	87000	293000			
E11b	362000	84000	282000			
E12b	359000	81000	272000			
E13b	369000	92000	309000			
E1c	370000	93000	318000	370000	92000	313000
E2c	370000	93000	312000			
E3c	369000	92000	308000			
E4c	371000	93000	318000			
E5c	370000	92000	311000			
E6c	369000	91000	308000			
E7c	370000	92000	319000			
E8c	370000	93000	313000			
E9c	369000	92000	308000			
E10c	369000	92000	317000			
E11c	370000	93000	315000			
E12c	368000	90000	303000			
E13c	371000	93000	322000			

On models Eia (no pore pressure) the shortest run-out (E9a; FA: 32°) and longest run-out (E13a; FA: 21°) are around 100 m distant (Figure 2). On models Eib (pu: 0.5) and even more on models Eic (pu: 0.7) the run-out distances of the different models are less spread. This shows that the friction angle becomes thus less influential on the travel distance when pore pressure increases (Figure 2).

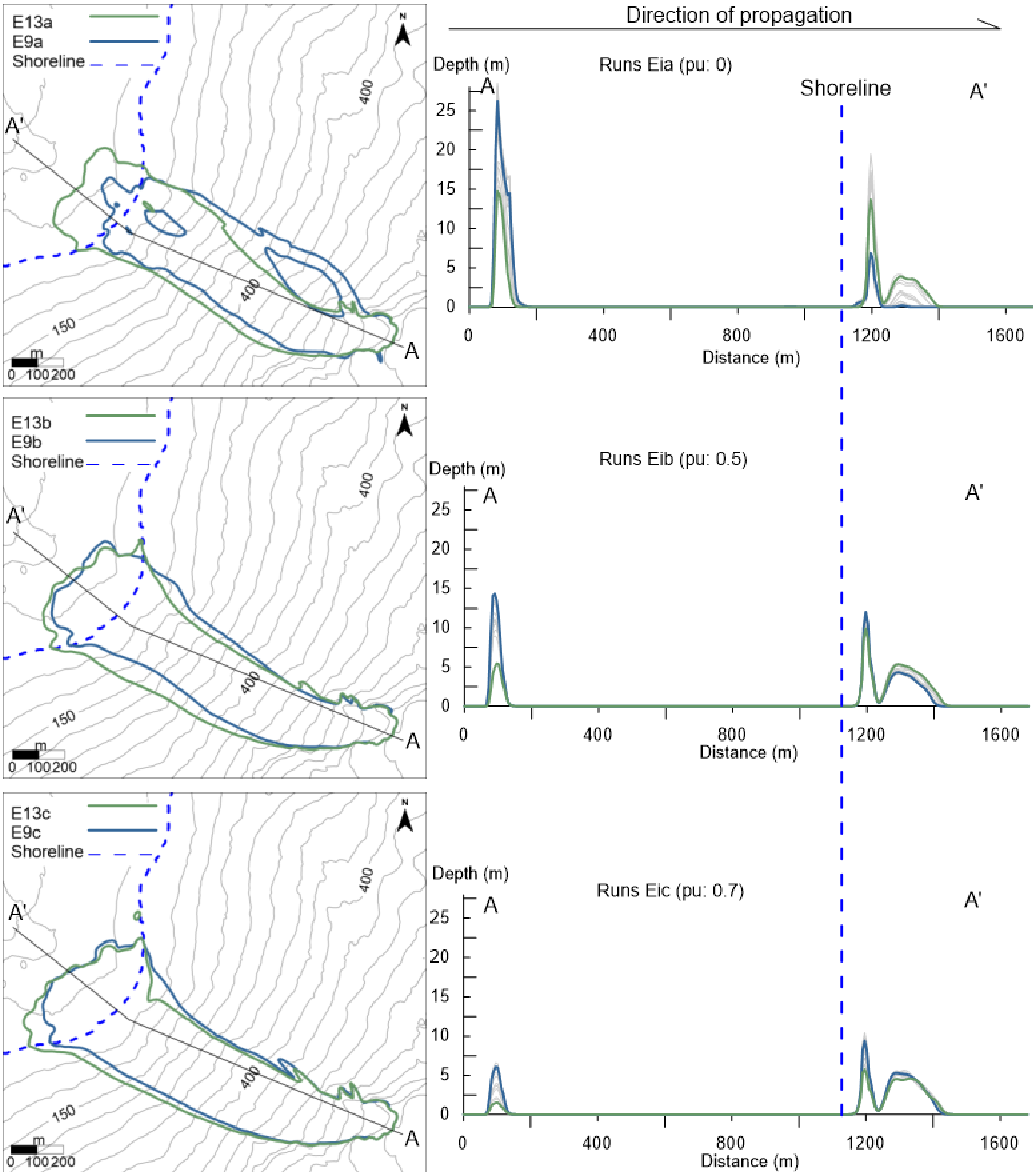

Figure 2. To the left: Dispersion of the rock mass involved in Stampa scenario 3A according to the pore pressure (pu) classes defined. To the right: Graphs showing depth of the rock mass at the end of the models and run-out distances for the different classes of pu considered. In colors we highlight the most extreme model runs (E9 and E13), and grey lines belong to the intermediate models. Note that spreading, and run-out distances increase with increasing pore pressure (pu), and that friction angle and internal friction angle have less impact on the final result with increasing pore pressure (less dispersion of results among the extreme models on Eib and Eic).

The entrainment of materials along the path topography increased the initial volume by ~30% on average. For the models with no pore pressure (Eia), the average final volume obtained was 334000 m^3. On these models around one third of the final volume was deposited in the fjord floor; the majority rested on the slope. In the models with higher saturation, the average final volume was 370000 m^3. On models Eib and Eic, the amount of materials deposited in the fjord floor was equal or higher than the initial volume (Table 2).

In all of the models, some materials remained in the source area. This was in part, a topographic effect (curvature of the sliding surface on its lower part), but primarily influenced by the input parameters. More material remained in the source area on those models with lower pore pressure and higher friction angles (e.g. E9a; Figure 2).

4.2 Propagation probability

In order to determine the area that would be most likely affected by the failure of Stampa scenario 3A, we built a propagation probability map with the results of the 39 model runs (Figure 3). The propagation area is around 1400 m long, starting at Joasetbergi and ending at -80 m depth in Aurlandfjord. The maximum propagation area has a width of ca. 600 m at the shoreline; the highest probability measures around 300 m at the shoreline. On the fjord floor, the rock mass propagates for about another 300 m. There are no houses on the propagation area, but the road E16, and a power line are positioned on the impact area.

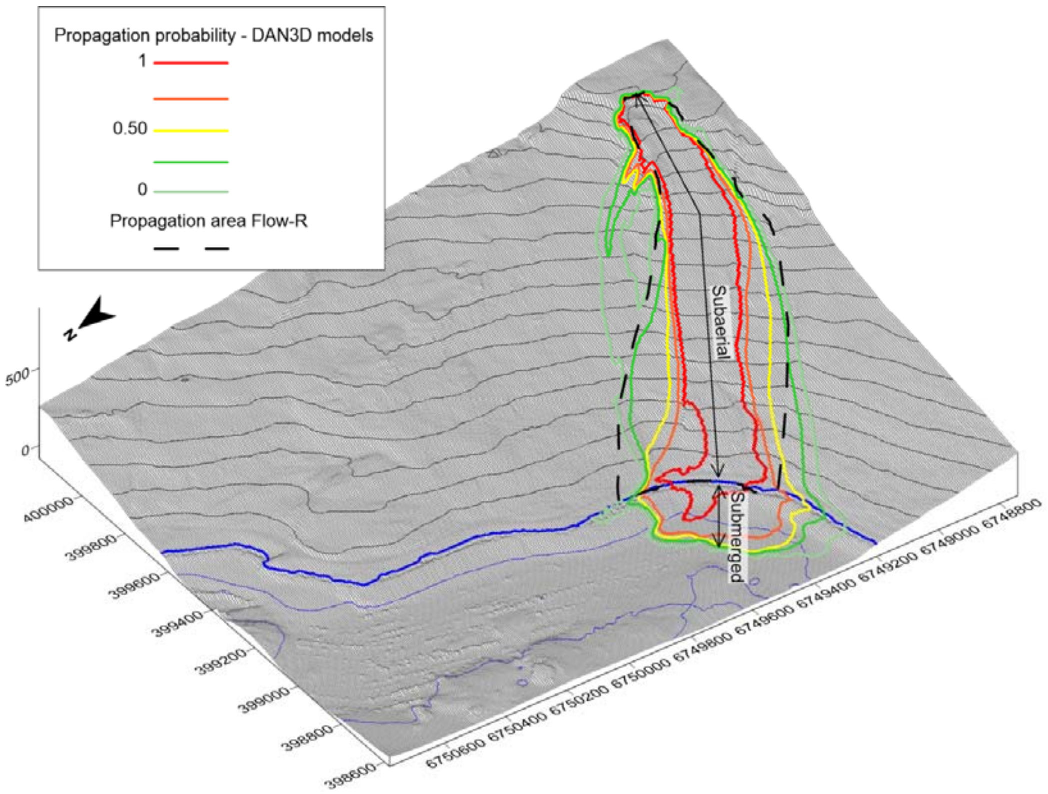

Figure 3. Probability of propagation for the 39 models considered and area modeled with Flow-R. Area modelled with Flow-R is cut to the shoreline, with no modelling of run-out for the submerged sector.

4.3 Propagation and impact velocities

The results of our models show that velocities increased with increasing pore pressure, and that higher velocities are reached on the central part of the propagation area (Figure 4). At the time of impact, models with no pore pressure (Eia) reached velocities of up to 35 m/s (average up to 20 m/s), models Eib reached velocities of up to 60 m/s (average up to 40 m/s) and models Eic reached velocities up to 70 m/s (average up to 55 m/s; Figure 4).

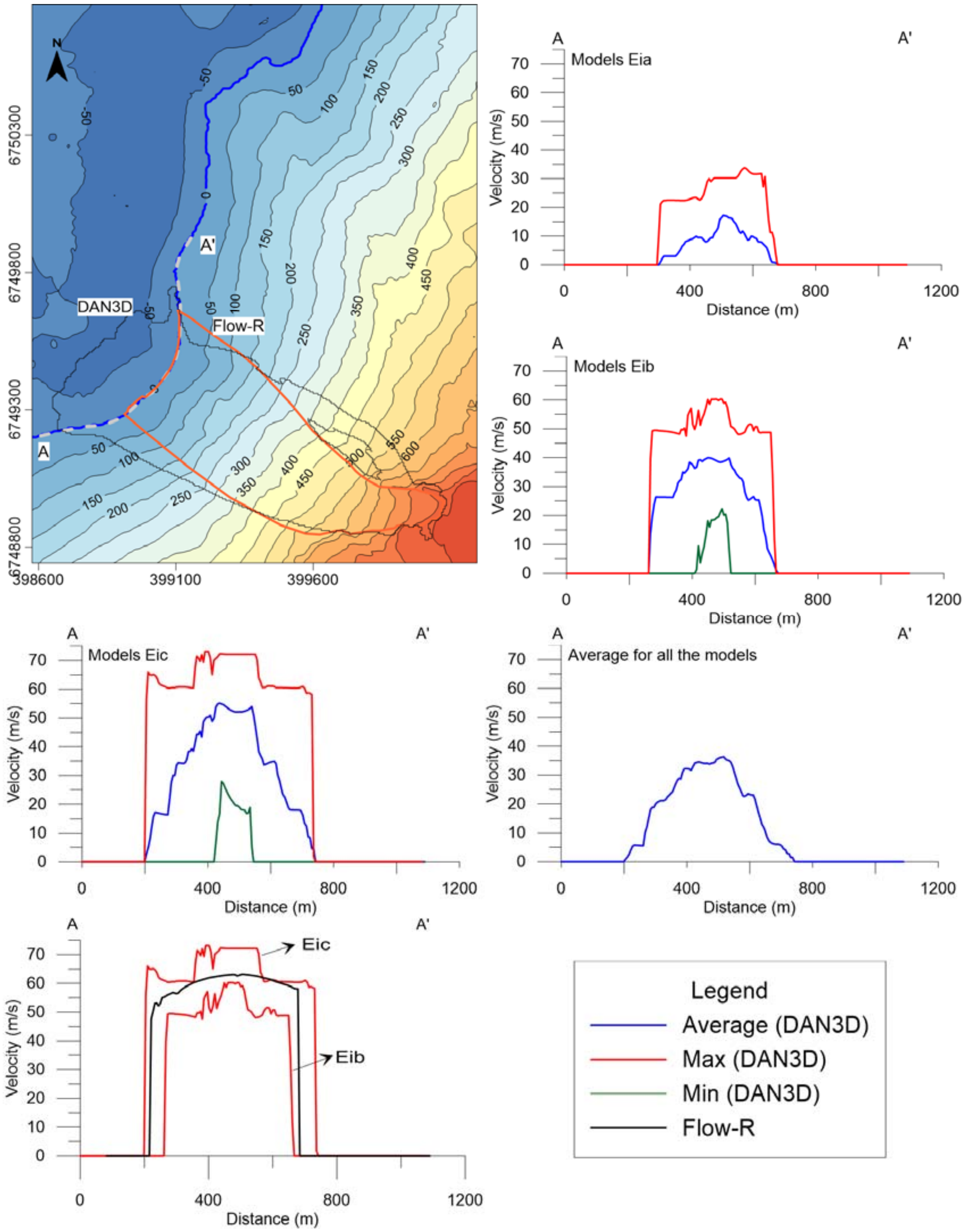

Figure 4. Contour map with propagation polygons obtained with DAN3D and Flow-R and graphs showing maximum, average and minimum velocities at the time of impact for the models Eia, Eib, and Eic (profile along the shoreline), as well as the average velocity at the time of impact for all the models. The bottom-left graph compares the maximum velocities obtained with the Eib and Eic models and the one with Flow-R.

Previous analyses done by NGU with VAW model and the Flow-R software showed impact velocities in the order of 60 m/s (216 km/h); a value that is not so close to the up to 40 m/s obtained by averaging the results of the 39 models. However, the value matches well with maximum velocities obtained in the models Eib and Eic that ranges between 50-70 m/s (Figure 4).

5. DISCUSSION AND CONCLUSIONS

The DAN3D software has been proven a reliable tool to simulate landslide propagation. It provided us with valuable information about the extension and dynamics of the rock mass in case of the failure of Stampa scenario 3A, and allowed us to validate previous results. In addition, the outputs of the models, such as width, length, thickness, and velocity of the rock mass at the time of impact, are key input data for future numerical modelling of displacement waves.

The dynamic run-out models with DAN3D showed the propagation of materials down to the fjord floor (to 80 m b.s.l.). The impact velocity would be in the order of 50-70 m/s. Scenarios with higher pore pressure coefficients and lower friction angles presented longer run-outs and higher propagation velocities. Considering the outcomes of the study done by Kristensen and Anda (2016) regarding the higher displacement rates during snowmelt season and heavy rainfall events, we conclude that the scenarios involving pore pressure (Eib and Eic) are most likely better reflecting the real conditions of a collapse compared to the dry condition models (Eia).

We overcame the lack of calibration of input parameters by defining 39 plausible propagation models. We compared their results with the ones obtained with two other independent models (Flow-R and VAW). Flow-R is an empirical model for regional susceptibility assessments of gravitational hazards developed by Horton et al., (2013) and is used by NGU for most of the unstable slopes in Norway. Flow-R, based on different spreading algorithms and frictional laws, determines the propagation of a source and the kinetic energy involved in its propagation, which can be converted to velocity. The VAW model (Heller et al., 2009) allows, among other things, to estimate the impact velocity of the rock mass producing a displacement wave. This model depends mainly on the morphometry of the unstable rock mass, the distance between its center of gravity and the shoreline, and the dynamic bed friction angle (Oppikofer et al., 2016). The Norwegian Geotechnical Institute (NGI) has previously carried out an analysis of the displacement waves that could be generated by the failure of the scenario 3A by using the PCM model (Perla et al., 1980) and considering a smaller initial volume (200000 m^3) and no entrainment. We summarize below the main conclusions that arise after comparing our results with previous analyses:

- The probability of propagation map produced with the results of DAN3D shows a good match with the propagation obtained with the Flow-R model.
- The distance between the shoreline and the distal part of the propagation area is around 300 m, shorter than the 400 m obtained previously by Domaas and Glimsdal (2009).
- The maximum impact velocities at the shoreline for scenarios of propagation Eib and Eic approximate well the one obtained with Flow-R, and with the VAW method. In addition, maximum velocities obtained with higher pore pressure coefficient are similar to the estimated velocities for historical rock avalanches in others mountain settings (see Sosio et al., 2008). The velocity at the impact estimated by NGI was 40 m/s (Domaas and Glimsdal, 2009), similar to the one obtained in the Eia models ("dry" models). The lower velocity could relate to the smaller volume used in their models.

Because of entrainment, the initial volume increased up to 371000 m^3. It has to be pointed out that DAN3D does not consider volumetric expansion of materials owing to rock fragmentation, which can increase the volume by 25% (Hungr and Evans, 2004). The volume deposited into the fjord turned out to be significant, being equal or higher than the estimated volume involved in Stampa scenario 3A. There is a dense vegetation coverage in the slope below 950 m a.s.l., which could, in case of failure, change the volume and the dynamics of the rock mass (e.g. friction, roughness, etc.). These effects of vegetation were not assessed in this work.

Even though erosion of sediments may also occur in the submerged part of the run-out area, it was neglected because of the uncertainty on the sedimentary cover (if any) on that section of the fjord. We therefore cannot evaluate how the eventual entrainment of submerged sediments would influence (in case it does) the magnitude of the triggered displacement waves.

6. MAIN REMARKS AND RECOMMENDATIONS

The results obtained with DAN3D are similar to those obtained in previous studies, and validate the propagation area of the Stampa scenario 3A delimited previously by NGU (NGU, 2017).

The collapse of Stampa scenario 3A would produce a rock avalanche deposit in Aurlandfjord, whose dimensions would depend on the entrainment and mobility of the rock mass. Therefore on the conditions of the slope at the time of failure.

The maximum final volume estimated was 371000 m^3. The impact velocity was estimated in ca. 50-70 m/s.

It is important to note that even if DAN3D can predict the propagation of rapid landslides with a certain degree of precision, the accuracy of the models could be improved if more interactions between the detached rocks and the substratum are addressed (e.g. effects of vegetation or snow cover, and underwater entrainment). Adding such information would improve the selection of some of the input parameters (i.e. friction, pore pressure, erosion), and therefore better approximate the real behavior of the rock mass.

There is a lack of knowledge of the parameters controlling the mobility of large-scale rockslides that fall into water bodies from back analyses. Because Norwegian fjords keep outstanding records of several of these events, their use in back analyses could help to overcome, at least partially, the lack of knowledge and would lead to more realistic scenarios in the Norwegian context.

7. REFERENCES

Blikra, L.H., Longva, O., Braathen, A., Anda, E., Dehls, J.F., and Stalsberg, K., 2006. Rock Slope Failures in Norwegian Fjord Areas: Examples, Spatial Distribution and Temporal Pattern, in: Evans,S.G., Scarascia Mugnozza,G., Strom, A. and Hermanns,R.L. (Eds.), Landslides from Massive Rock Slope Failure; NATO Science Series, IV. Earth and Environmental Sciences, v. 49. Springer, Dodrecht, Netherlands, pp. 475-496.

Blikra, L.H., Böhme, M., Dehls, J., Hermanns, R.L., Oppikofer, T., Redfield, T., Rønning, J.S., Yugsi Molina, F., Domaas, U., Pfaffhuber, A., Henriksen, H., Hole, J., and Kristensen, L., 2013. The unstable phyllitic rocks in Stampa - Flåm, western Norway: Compilation, scenarios, risk and recommendations. NVE report no. 35-2013, Norwegian Water Resources and Energy Directorate, Oslo, Norway.

Blikra, L.H., Braathen, A., Anda, E., Stalsberg, K. and Longva, O., 2002. Rock avalanches, gravitational bedrock fractures and neotectonic faults onshore northern West Norway: Examples, regional distribution and triggering mechanisms. NGU report no. 2002.016, Geological Survey of Norway, Trondheim, Norway.

Blikra, L.H., Majala, G., Anda, E., Berg, H., Eikenæs, O., Helgås, G., Oppikofer T., Hermanns, R., and Böhme, M., 2016. Fare-og risikoklassifisering av ustabile fjellparti. Faresoner, arealhandtering og tiltak. NVE report no. 77-2016, Norwegian Water Resources and Energy Directorate, Oslo, Norway.

Böhme, M., Hermanns, R.L., Oppikofer, T., Fisher, L., Bunkholt, H.S.S., Eiken, T., Pedrazzini, A., Derron, M.-H., Jaboyedoff, M., Blikra, L.H., and Nilsen, B., 2013. Analysing complex rock slope deformation at Stampa, western Norway, by integrating geomorphology, kinematics and numerical modelling. Engineering Geology, v. 154, 116-130.

Braathen, A., Blikra, L.H., Berg, S.S., and Karlsen, F., 2004. Rock-slope failure in Norway; type, geometry, deformation mechanisms and stability. Norwegian Journal of Geology, v. 84, no. 1, 67-88.

Domaas, U., Rosenvold, B.S., Blikra, L.H., Johansen, H., Grimstad, E., Sørlie, J.E., Gunleiksrud, O., Engen, A., and Lægreid, O., 2002. Studie av fjellskred og dalsidestabilitet i fyllittområder (Report to the Norwegian Research Counsil). NGI report no. 20001132-32, Norwegian Geotechnical Institute Report, Oslo, Norway.

Domaas, U., and Glimsdal, S., 2009. Skred og flodbølger ved Flåm, Aurland kommune. NGI report no. 20081693-1, Norwegian Geotechnical Institute, Oslo, Norway.

Harbitz, C.B., Glimsdal, S., Løvholt, F., Kveldsvik, V., Pedersen, G.K., and Jensen, A., 2014. Rockslide tsunamis in complex fjords: From an unstable rock slope at Åkerneset to tsunami risk in western Norway. Coastal Engineering, v. 88, 101-122.

Heller, V., Hager, W.H., and Minor, H.E., 2009. Landslide generated impulse waves in reservoirs. VAW Mitteilungen 211, Laboratory of Hydraulics, Hydrology and Glaciology (VAW), ETH Zurich: Zurich, Switzerland.

Hermanns, R.L., Fischer, L., Oppikofer, T., Böhme, M., Dehls, J.F., Henriksen, H., Booth, A., Eilertsen, R., Longva, O., and Eiken, T., 2011. Mapping of unstable and potentially unstable slopes in Sogn og Fjordane (work report 2008-2010). NGU report no. 2011.55, Geological Survey of Norway, Trondheim, Norway.

Hermanns, R.L., Oppikofer, T., Böhme, M., Dehls, J., Yugsi-Molina, F., and Penna, I.M., 2016. Rock slope instabilities in Norway: First systematic hazard and risk classification of 22 unstable rock slopes from northern, western and southern Norway. In: Aversa, S., Cascini, L., Picarelli,L., and Scavi, C. (Eds). Landslides and Engineered Slopes. Experience, Theory and Practice - Proceedings of the 12th International Symposium on Landslides, pp.1107-1114

Horton, P., Jaboyedoff, M., Rudaz, B., and Zimmermann, M., 2013. Flow-R, a model for susceptibility mapping of debris flows and other gravitational hazards at a regional scale. Natural Hazards and Earth System Sciences, v. 13, 869-885.

Hungr, O., and Evans, S.G., 2004. Entrainment of debris in rock avalanches: an analysis of a long run-out mechanism. Geological Society of America Bulletin, v. 116, 1240-1252.

Hungr, O., and Evans, S.G., 1996. Rock avalanche runout prediction using a dynamic model. In: Senneset, K. (Ed.). Proceedings of the 7th International Symposium on Landslides, Trondheim, Norway, v. 1, 233-238.

Hungr, O., and McDougall, S., 2009. Two numerical models for landslide dynamic analysis. Computers & Geosciences, v. 35, 978-992.

Kristensen, L., and Anda, E., 2016. Bakkebaserte radarmålinger på Børa i Romsdalen og Stampa ved Flåm. NVE report no. 84-2016, Norwegian Water Resources and Energy Directorate, Oslo, Norway.

Mazzati, P., and Bozzano, F., 2011. Revisiting the February 6th 1783 Scilla (Calabria, Italy) landslide and tsunami by numerical simulation. Marine Geophysics Research, v. 32, 273-286.

Mazzati, P., Bozzano, F., Avolio, M.V., Lupiano, V., and Di Gregorio, S., 2010. 3D Numerical Modelling of Submerged and Coastal Landslide Propagation. Advances in Natural and Technological Hazards Research, v. 28, 127-139.

McDougall, S., and Hungr, H., 2004. A model for the analysis of rapid landslide motion across three-dimensional terrain. Canadian Geotechnical Journal, v. 41, 1084-1097.

NGU, 2017. Nasjonal database for ustabile fjellparti. http://geo.ngu.no/kart/ustabilefjellparti/ Geological Survey of Norway, Trondheim, Norway.

Oppikofer, T., 2009. Dectection, analysis and monitoring of slope movements by high-resolution digital elevation models. Ph.D. thesis. Institute of Geomatics and Analysis of Risk, University of Lausanne, Switzerland.

Oppikofer, T., Böhme, M., Nicolet, P., Penna, I., and Hermanns, R.L., 2016. Metodikk for konsekvensanalyse av fjellskred. NGU report no. 2016.047, Geological Survey of Norway, Trondheim, Norway.

Penna, I.M., Derron, M.-H., Volpi, M., and Jaboyedoff, M., 2013. Analysis of past and future dam formation and failure in the Santa Cruz River (San Juan province, Argentina). Geomorphology, v. 183, 28-38.

Perla, R., Cheng, TT., and McClung, D.M., 1980. A two-parameter model of snow-avalanche motion. Journal of Glaciology, v. 26, 197-207.

Schleier, M., Hermanns, R.L., Gosse, J.C., Oppikofer, T., Rohn, J., and Tønnesen, J.F., 2016. Subaqueous rock-avalanche deposits exposed by post-glacial isostatic rebound, Innfjorddalen, Western Norway. Geomorphology, in press. doi: 10.1016/j.geomorph.2016.08.024

Sosio, R., Crosta, G.B., and Hungr, O., 2008. Complete dynamic modeling calibration for the Thurwieser rock avalanche (Italian Central Alps). Engineering Geology, v. 100, 11-26.

GEOLOGICAL
SURVEY OF
NORWAY
- NGU -

Geological Survey of Norway
PO Box 6315, Sluppen
N-7491 Trondheim, Norway

Visitor address
Leiv Eirikssons vei 39
7040 Trondheim

Tel (+ 47) 73 90 40 00
E-mail ngu@ngu.no
Web www.ngu.no/en-gb/